MODELING OF THE RESIN VISCOELASTICITY IN THE FORMING PROCESS OF THERMOPLASTIC COMPOSITES

Qi Wu[1, 2], Tomotaka Ogasawara[1], and Nobuhiro Yoshikawa[1]

[1] Institute of Industrial Science, the University of Tokyo, 4-6-1 Komaba, Meguro-ku, Tokyo 153-8505, Japan
[2] State Key Laboratory of Mechanics and Control of Mechanical Structures, Nanjing University of Aeronautics and Astronautics, Yudao Street 29, Nanjing 210016, China

Keywords: Viscoelasticity. Amorphous polymer, Carbon fiber reinforced thermoplastic, shift factor

ABSTRACT

Viscoelasticity analysis plays a key role in forming process of carbon fiber reinforced thermoplastics (CFRTPs) because it enables precise prediction of the residual stress caused by resin shrinkage and thermal expansion mismatch. A program integrated with a new shift factor model was developed to interpret the resin viscoelasticity data from dynamic mechanical analysis, then plot the corresponding master curve, and subsequently give a self-consistent spring-dashpot model of the resin. This technique has potential to be encoded into a finite element analysis software to predict the residual stress in a micro-model of a CFRTP consisting of carbon fiber and thermoplastic resin.

1 INTRODUCTION

Carbon fiber reinforced thermoplastics (CFRTPs), a kind of cutting-edge composite materials, have drawn increasing attentions from both academia and industry owing to its unique advantage of highly efficient production compared to thermosetting composite. In order to achieve short moulding time, the preheated CFRTP is press-moulded and then rapidly cooled to the service temperature. Such manufacture procedure could easily result into considerable residual strain and stress in the CFRTP after demoulding, because of residual stress formation on three mechanical level from micro, through macro, to global [1]. Understanding mechanism of residual stress in the micro level benefits other two-levels researches. In the micro level, the residual stress caused by the thermoplastic resin shrinkage and mismatch of coefficient of thermal expansion between the reinforcement and matrix will be partially released due to the viscoelasticity of the resin. Without considering the material modulus in the time-temperature scenario, the modelling of forming process of CFRTP will generally overestimate the laminate deformation [2]. Thus, it is important to precisely model the resin viscoelasticity though it is difficult.

Dynamic mechanical analysis (DMA) running in temperature-sweeping and frequency-sweeping modes is a standard technique to obtain material's temperature-dependent and frequency-dependent moduli. Although both properties are vital to material researchers, they exist intrinsic interrelation and could be inter-converted to plot a master curve according to the well-known principle that is time-temperature superposition [3]. However, connecting multiple temperature-dependent moduli (or the frequency/time-dependent moduli) via shift factor to plot a smooth and rational master curve covering long time duration is considerably different [4]. Even assuming the viscoelasticity is linear and following Boltzmen superposition principle, different resins maybe process distinguishing shift factors [5]. Arrhenius (Arr) and Williams–Landel–Ferry (WLF) models are widely used but have limited applicable ranges. Direct data process method, such as least-square, can fit the data in various cases albeit with no physical meaning. Combining Arr and WLF models though glass transition temperature is one feasible way [6]. Cascading two Arr models is another possible way [7]. Various other complex models aiming at different materials are also proposed by researchers [8].

Anther common challenge in viscoelasticity research is the modelling method of the master curve. Based on the concept of connecting multiple spring-dashpot elements in series or in parallel, generalized Maxwell and Voigt models could describe the master curve. In mathematics, these two models are achieved by using Prony series to fit to the master curves of modulus and compliance [9].

For the sake of time- and cost- saving, usually only modulus or compliance is measured, while leaving the other to be calculated. Since viscoelasticity is the modulus about time, converting modulus into compliance cannot be simply calculated as reciprocal, and vice versa [3, 4]. Therefore, how to automatically convert modulus model to compliance model is another issue the authors will address in this research.

The viscoelasticity of the polyetherimide (PEI) resin, one kind of amorphous thermoplastics that can be used in CFRTP, was investigated in this paper. The authors developed a program package, which can smartly extract the useful information from the DMA data and then present the master curve, as well as propose the self-consistent viscoelasticity model. The results were validated by another set of experiment data, and will benefit the following forming simulation of CFRTP.

2 PEI VISCOELASTICITY

The PEI resin used in this research was manufactured by Mitsubishi Plastics, Inc, and two sets of DMA tests were conducted to acquire its mechanical properties. The first dataset contains both elastic and shear moduli obtained from temperature-sweeping mode, and the second dataset has only elastic modulus obtained from frequency-sweeping mode. Without specific indication, the following presented results were from the first data set, while the second dataset was used as the reference. The output of DMA test is the dynamic moduli, including the storage modulus E', loss modulus E'', the phase lag δ. Eqs. 1 and 2 show the relation among these three parameters.

$$E' = E\cos\delta \tag{1}$$

$$E'' = E\sin\delta \tag{2}$$

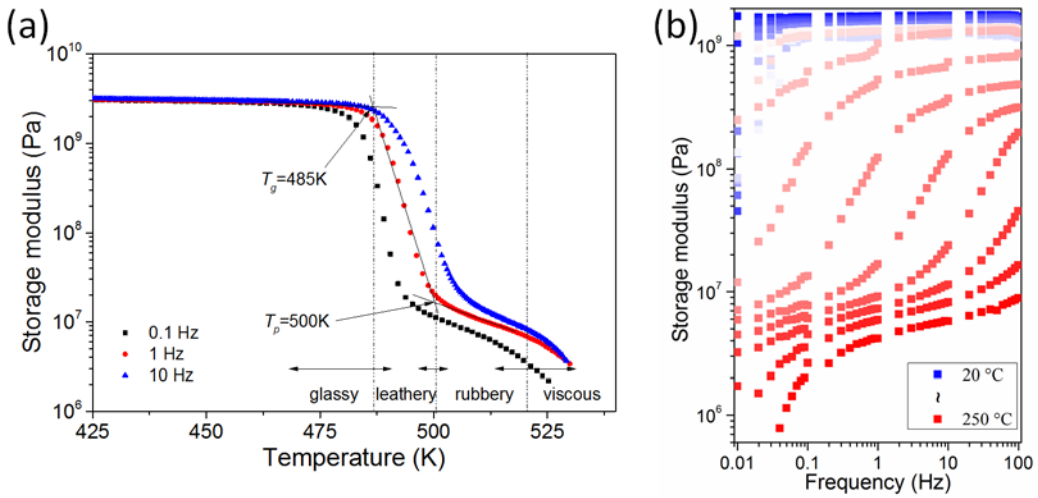

Figure 1: Storage modulus of the PEI resin. (a) Temperature-dependent E' obtained from temperature sweeping mode; (b) frequency-dependent E' obtained from frequency sweeping mode.

Figure 1(a) shows the temperature-dependent E' in 0.1,1 and 10 Hz. There are two key temperatures in the 1-Hz E' curve. The glass transition temperature T_g of the PEI resin is approx. 485 K, and T_p, the temperature when the rubbery plateau begins to form, is approx. 500 K. Usually the temperature-dependent curve can be roughly divided into four distinct stages that are glassy, leathery, rubbery and viscous based on different material properties. In the glassy stage, the stiffness of the resin is high and does not degenerate a lot. In the leathery stage, namely glass transition stage, stiffness decreases thousand times rapidly when the temperature is over T_g. After T_p, a rubbery plateau forms, and then is the viscous stage when temperature further increases. Because this PEI sample is not crosslinked polymer, its rubbery plateau has very limited range, quickly followed by a further decrease of the stiffness in the viscous stage. Owning to the indistinguishable rubbery-viscous stage, the storage modulus of the PEI resin also can be divided into three stages — glassy, leathery, and rubbery-viscous.

Figure 1(b) shows the frequency-dependent E' from the second set of data in 20 - 250 °C. Because the very hot laminate cools down to service temperature (room temperature) in the actual forming process of CFRTP, the master curve interpreted from the temperature-dependent modulus (or frequency-dependent modulus) should cover tremendous time range. It means that the master curve should be smooth and contain all the information shown in Fig. 1(a) or (b). We tried and found neither conventional Arr model, conventional WLF model nor blending Arr-WLF model can precisely shift the segmented time-temperature-dependent E' to form a complete and smooth master curve. Therefore, a novel and specific shift factor model is urgently needed.

3 SHIFT FACTOR AND MASTER CURVE

3.1 Arrhenius model with alterable activation energy

Eq. 3 is the blending Arr and WLF model used in [6].

$$\begin{cases} \log_{10} A_T^1 = \dfrac{E_{act}}{\ln(10)R}\left(\dfrac{1}{T}-\dfrac{1}{T_0}\right) & \left(T \le T_g\right) \\ \log_{10} A_T^2 = A_T^1 \dfrac{-C_1\left(T-T_g\right)}{C_2+\left(T-T_g\right)} & \left(T > T_g\right) \end{cases} \tag{3}$$

where A_T is the shift factor, E_{act} is the activation energy, R is the universal gas constant, T_0 is the reference temperature, C_1 and C_2 that are the empirical constants in the WLF model are typically set to 17.44 and 51.6, respectively. The blending model is used as the reference in the following research.

Unlike Eq. 3 that only uses T_g as the key point to connect Arr model and WLF model, our new model has simple Arrhenius format. But its E_{act} is alterable according to different temperature ranges divided by T_g and T_p. Eq. 4 is the expression.

$$\begin{cases} \ln A_T^1 = \dfrac{E_1}{R}\left(\dfrac{1}{T}-\dfrac{1}{T_0}\right) & T < T_g \\ \ln A_T^2 = A_T^1 \dfrac{E_2}{R}\left(\dfrac{1}{T}-\dfrac{1}{T_g}\right) & T_g < T < T_p \\ \ln A_T^3 = A_T^2 \dfrac{E_3}{R}\left(\dfrac{1}{T}-\dfrac{1}{T_p}\right) & T_p < T \end{cases} \tag{4}$$

where E'_{act} are the activity energy in the different stages. The physical meaning of different E_{act} could be explained as the behavior change of the secondary bonds in a resin [10]. In the glassy stage, the secondary bonds stretch when temperature increases. This phenomenon occurs in the temperature lower than T_g and needs relatively low E_{act}. When temperature is over T_g, the secondary bonds begin to break, leading to sliding of the molecules. Thus, E_{act} required is high, and the modulus drops dramatically in the leathery stage followed by a plateau where the molecules may still remember their original positions. Then, almost all the secondary bonds break as the temperature further increases. Consequently, all molecules can move freely and the modulus drops again, corresponding to the rubbery-viscous stage after T_p.

3.2 Comparison of shift factors

In both Eqs. 3 and 4, activation energy should be determined respecting the specific material. We have tried to calculate it based on the equations used in [11], but found the results were inappropriate. We, therefore, used a sophisticated mathematical way to get this parameter, as shown in Fig. 2. After the range of the E_{act} is determined roughly, multiple master curves could be plotted when one E_{act} is

used. Every master curve is smoothed by using Savitzky-Golay method, and its correlation coefficient is calculated to evaluate the smoothness, namely the quality of master curve. Among the multiple correlation coefficients, the most suitable value can be found and lastly to reversely trace the optimal E_{act}.

Figure 3 shows the shift factors obtained from Eq. 2, Eq. 3, and direct fitting [7, 12]. The T_0 in this figure and all hereinafter master curves are set to 160 °C. The direct fitting is largely different to the rest two methods. Its consequent master curve is obviously incorrect. The first and second ways show nearly the same shift factor when temperature is lower than T_g since their evaluated E_{act} is similar. These two curves do not overlap when temperature is higher than T_g, as shown in the inset. T_p further separates the shift factor curve, which is calculated from the modified Arr model, into two parts.

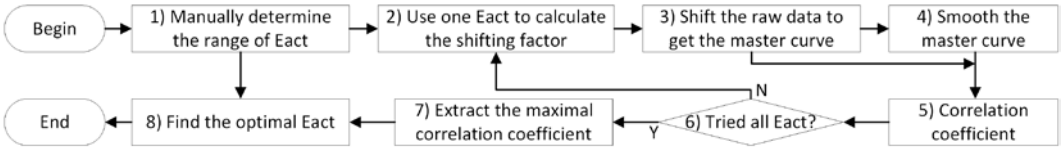

Figure 2: Flow chart of the data process to determine the activation energy in the Arrhenius model.

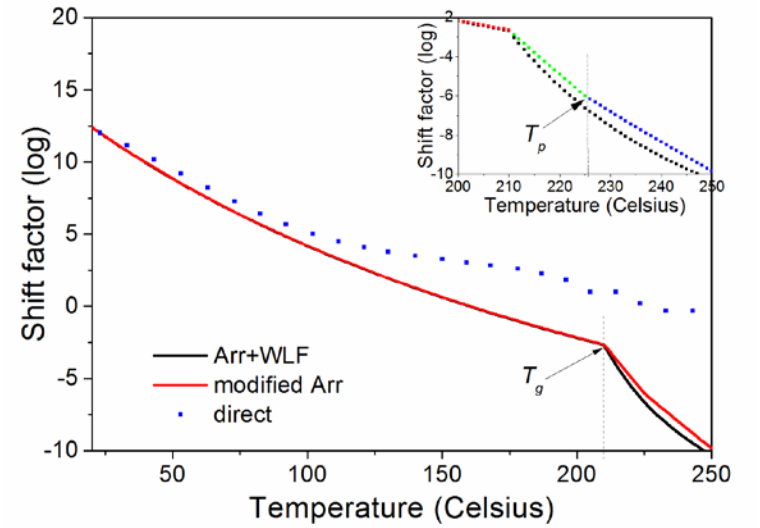

Figure 3: Comparison among different shift factors. Inset shows the detail of shift factors in high temperature.

3.3 Master curves

Figure 4(a-b) compares the master curves of E' obtained by using blending method (Eq. 3) and modified Arr method (Eq. 4). Both master curves cover similar frequency range and show the change of E'. Although both curves are relatively smooth, the master curve in Fig. 4(b) has a noticeable bifurcation in the range of 10^{-13} - 10^{-8} Hz, marked as a circle in Fig. 4(b). The dots in this frequency range are shifted from the dots in high temperature, especially when temperature is over T_p. It means that straightforward usage of WLF model in the temperature over T_g is inappropriate at least to this PEI resin. We have demonstrated that the bifurcation also appears when we used the blending method to calculate the master curve of G'. On the other hand, the E'', G' and G'' calculated by the modified Arr method are smooth, as shown in Fig. 4(c-d). Thus, it demonstrated that the shift factor calculated by the new method is universal to all dynamic moduli of the PEI resin. It is also believed that the newly proposed modified Arr method is superior to previous model if tremendous frequency range is needed, though it should be tested to more different resins in the future research.

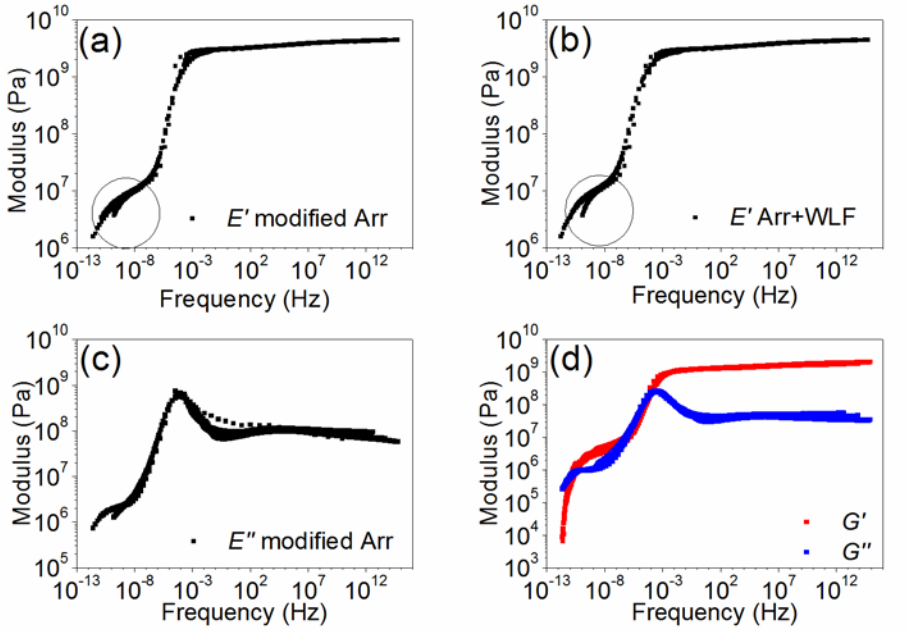

Figure 4: Master curves. (a) E' calculated by modified Arr method; (b) E' calculated by blending method; (c) E'' calculated by modified Arr method; (d) G' and G'' calculated by modified Arr method.

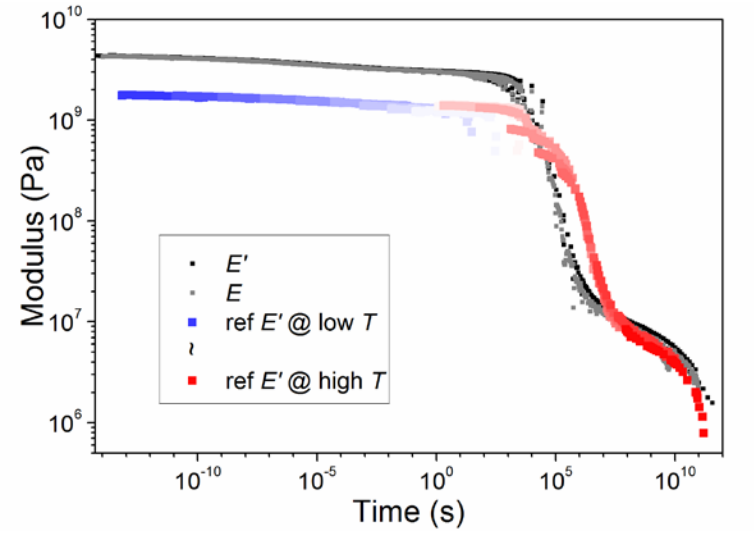

Figure 5: Time-dependent elastic modulus.

3.4 Time-dependent elastic modulus

Eq.5 is used to approximate the transient modulus from the dynamic moduli [13].

$$E(t) = E'(\omega) - 0.4E''(0.4\omega) + 0.014E''(10\omega)\Big|_{\omega=1/t} \tag{5}$$

where ω is the frequency in radians per second. It can be simplified to Eq. 6 because of the small loss modulus compared to the large storage modulus of the PEI resin, as shown in Fig. 4(a) and (c).

$$E(t) = E'(\omega)\Big|_{\omega=1/t} \tag{6}$$

In Figure 5, the high similarity between the gray and black dots calculated by Eqs. 5 and 6 demonstrates the correctness of the simplification from Eq. 5 to Eq. 6. A series of dots changing color from blue to red is the master curve calculated by the second dataset. This master curve has similar

trend to that one from the first dataset. However, the values of these two experimental datasets are different. Referring to the elastic modulus of 3075 MPa obtained from a standard tensile test (this value is provided by the PEI manufacturer), the curves shown in Fig. 5 have a certain level of error. This mismatch is probably resulted from different experiment conditions, but needs further verification.

4 MODEL OF THE MODULI

4.1 Generalized Maxwell model

Spring-dashpot element is the fundamental concept to model the material viscoelasticity. Eq. 7 is the expression of generalized Maxwell model consisting of several Maxwell elements assembled in parallel [14], and Eq. 8 is the expression of generalized Voigt model consisting of several Voigt elements assembled in series.

$$E(t) = E_\infty + \sum_{i=1}^{n} E_i \left(e^{-t/\tau_i} \right) \tag{7}$$

$$D(t) = D_0 + \sum_{j=1}^{n} D_j \left(1 - e^{-t/\tau_j} \right) \tag{8}$$

where E_∞ is the long term modulus, D_0 is the instantaneous compliance, E_i and D_j are the modulus and compliance associated with each spring-dashpot element, τ_i and τ_j are relaxation and retardation time, respectively. Maxwell model and Voigt model are suitable to describe stress relaxation phenomenon and creep phenomenon, respectively. Although these two equations are different, they both have exponential decay format and could be fitted to Prony series. We provide two data process methods. In the method shown in Fig. 6(a), both E_i and τ_i are determined by using nonlinear least-square method to fit to a 3-terms Prony series. In the second method shown in Fig. 6(b), 13-terms Prony series, in which τ_i is predetermined, is used and then only E_i is calculated. Fig. 6(b) fits the original master curve better because more terms are used. The reason to predetermine τ_i is because of the considerably long time the data process will cost if setting both E_i and τ_i to be variable. We also found that by predetermining τ_i with the format of 10 power the result is reliable and very precise. However, the fitting curve in Fig. 6(a) is roughly honest to the trend of the master curve. Considering its relatively simple expression, the following FEA was conducted based on this 3-terms Prony series.

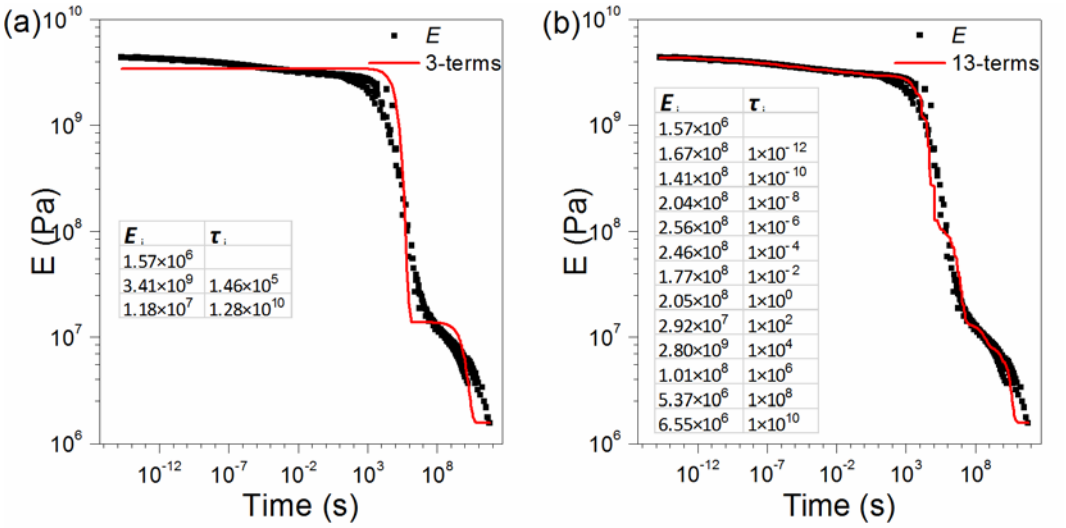

Figure 6: Master curves and their corresponding Prony series fitting curves. (a) 3-terms Prony series fit to E ; (b) 13-terms Prony series fit to E by using predetermined relaxation time. The tables inserted are the relevant parameters.

4.2 Maxwell and Voigt model interconversion

Conversion from Maxwell model to Voigt model, or reversely, is substantially difficult. Herein we deduce the mathematical conversion from Maxwell to Voigt model. Eq. 9 is the Laplace-domain expression of Eq. 7. Eq. 10 is the interrelation between Maxwell and Voigt model in Laplace-domain, i.e., the relation between modulus and compliance. By substituting Eq. 9 into Eq. 10, compliance in Laplace-domain $D(s)$ could be expression as a fraction, whose denominator and numerator both are polynomial. Eq. 11 can further be written as the accumulation of a series of fractions, in which α_i and β_i should be determined. α_i can be firstly calculated by solving the polynomial in the denominator, then β_i can be calculated by using partial fraction decomposition, such as residue method in our program. In the last step, Eq. 11 is inverse-Laplace transformed to get the compliance expression in time domain Eq. 12. The compliance curves shown in Fig. 7 corresponds to the modulus curves shown in Fig. 6, and the inset is the compliance curves in linear scale for reference. Both curves have similar time range and compliance magnitude, but 3-terms compliance increases later than 13-terms one.

$$E(s)=\frac{E_\infty}{s}+\sum_{i=1}^{n}\frac{E_i}{s+1/\tau_i} \tag{9}$$

$$D(s)=\frac{1}{E(s)s^2} \tag{10}$$

$$D(s)=\frac{p_n s^n+\square+p_2 s^2+p_1 s^1+p_0}{\left(q_n s^n+\square+q_2 s^2+q_1 s^1+q_0\right)s}=\sum_{i=0}^{n+1}\frac{\beta_i}{(s+\alpha_i)} \tag{11}$$

$$D(t)=\sum_{i=0}^{n+1}\beta_i e^{-\alpha_i t} \tag{12}$$

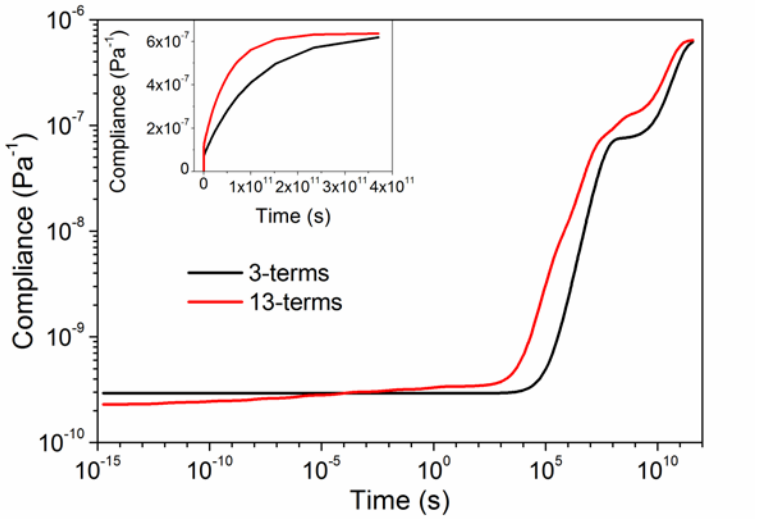

Figure 7: Compliance obtained by using Laplace transform. Inset shows the compliance in linear scale.

6 CONCLUSION

In this paper, the viscoelasticity of a PEI resin was researched comprehensively. A new shift factor model was proposed and a program package was developed to accomplish master curve and spring-dash model. The modeling results were validated by comparing to another experimental data. The originality of this research is highlighted as:

1) the viscoelasticity properties of the PEI resin were clarified;

2) the Arr model with alterable activation energy was newly proposed to perfectly obtain the master curve;

3) the automatic interconversion between Maxwell model and Voigt model was achieved by using Laplace transform with partial fraction decomposition method.

ACKNOWLEDGEMENTS

This work was supported by the grant from sub-category 8 entitled “Research and development of multiscale modelling simulators for thermoplastic CFRP” in Japan national project of next-generation supercomputer ‘Post-K’.

REFERENCES

[1] P. P. Parlevliet, H. E. Bersee, and A. Beukers, Residual stresses in thermoplastic composites—A study of the literature—Part I: Formation of residual stresses, *Composites Part A: Applied Science and Manufacturing*, **37**, 2006, pp. 1847-1857.

[2] C. Brauner, T. B. Block, and A. S. Herrmann, Meso-level manufacturing process simulation of sandwich structures to analyze viscoelastic-dependent residual stresses, *Journal of Composite Materials*, **46**, 2012, pp. 783-799.

[3] M. T. Shaw and W. J. MacKnight, *Introduction to polymer viscoelasticity*, John Wiley & Sons, 2005.

[4] J. D. Ferry, *Viscoelastic properties of polymers*, John Wiley & Sons, 1980.

[5] P. Dasappa, P. Lee-Sullivan, and X. Xiao, Temperature effects on creep behavior of continuous fiber GMT composites, *Composites Part A: Applied Science and Manufacturing*, **40**, 2009, pp. 1071-1081.

[6] M. Tajvidi, R. H. Falk, and J. C. Hermanson, Time–temperature superposition principle applied to a kenaf-fiber/high-density polyethylene composite, *Journal of applied polymer science*, **97**, 2005, pp. 1995-2004.

[7] Y. Miyano, M. Nakada, and H. Cai, Formulation of long-term creep and fatigue strengths of polymer composites based on accelerated testing methodology, *Journal of composite materials*, 2008.

[8] N. I. M. Yusoff, E. Chailleux, and G. D. Airey, A comparative study of the influence of shift factor equations on master curve construction, *International Journal of Pavement Research and Technology*, **4**, 2011, pp. 324-336.

[9] C. Tzikang, Determining a Prony series for a viscoelastic material from time varying strain data, NASA Langley Technical Report, 2000.

[10] C. Mahieux and K. Reifsnider, Property modeling across transition temperatures in polymers: a robust stiffness–temperature model, *Polymer*, **42**, 2001, pp. 3281-3291.

[11] W. K. Goertzen and M. Kessler, Creep behavior of carbon fiber/epoxy matrix composites, *Materials Science and Engineering: A*, **421**, 2006, pp. 217-225.

[12] K. Fukushima, H. Cai, M. Nakada, and Y. Miyano, Determination of time-temperature shift factor for long-term life prediction of polymer composites, in *Proc. ICCM 17*, .

[13] P. Hooper, B. Blackman, and J. Dear, The mechanical behaviour of poly (vinyl butyral) at different strain magnitudes and strain rates, *Journal of Materials Science*, **47**, 2012, pp. 3564-3576.

[14] A. V. Duser, A. Jagota, and S. J. Bennison, Analysis of glass/polyvinyl butyral laminates subjected to uniform pressure, *Journal of Engineering Mechanics*, **125**, 1999, pp. 435-442.